# Adsorption and Laser-Induced Thermal Desorption of 1,3-Butadiene on HOPG(0001)

**ARTICLE** *in* THE JOURNAL OF PHYSICAL CHEMISTRY B · SEPTEMBER 2002

Impact Factor: 3.3 · DOI: 10.1021/jp021196n

# Adsorption and Laser-Induced Thermal Desorption of 1,3-Butadiene on HOPG(0001)

**Jason K. Oman and Simon J. Garrett***

*Department of Chemistry, Michigan State University, East Lansing, Michigan 48824-1322*

*Received: May 14, 2002; In Final Form: July 31, 2002*

The adsorption and UV photochemistry of 1,3-butadiene ($CH_2$═$CHCH$═$CH_2$) on highly oriented pyrolytic graphite (HOPG(0001)) was studied using temperature-programmed desorption (TPD) and electron energy loss spectroscopy (EELS). Butadiene physisorbs on HOPG with the monolayer exhibiting first-order desorption kinetics and a corresponding desorption energy of 32 kJ/mol. The multilayer exhibits zero order desorption kinetics with a desorption energy of 28.5 kJ/mol. Irradiation of the $C_4H_6$/HOPG(0001) adlayer (one and three monolayers (ML) of $C_4H_6$) with UV photons at 193, 248, and 351 nm and fluences of up to 100 mJ/cm$^2$·pulse resulted in molecular photodesorption. Photodesorption was described by a laser-induced thermal desorption process as supported by simple calculations of the surface temperature rise. The photoprocesses occurring in both 1 and 3 ML $C_4H_6$ adlayers on HOPG(0001) were also investigated at incident powers of ≤10 mJ/cm$^2$·pulse. Under these conditions, there was no detectable photodesorption or condensed phase photochemistry at any of the wavelengths investigated.

## Introduction

During the past few decades, it has become clear that heterogeneous reactions on atmospheric aerosol surfaces play an important role in the chemistry of the troposphere and stratosphere. The majority of the research conducted to date has focused on understanding reactions on model stratospheric clouds, pure and acidified ice surfaces that participate in the catalytic cycles of reservoir species such as $ClONO_2$ and HOCl.[1−6] These reactions ultimately contribute to net stratospheric ozone destruction.[7−13] More recently, interest has shifted toward the potentially wider range of chemical and photochemical reactions in the troposphere that may be mediated by other aerosol surfaces. Particulates present in the atmosphere include those composed of sea-salt, metal oxide, aluminosilicates, and carbonaceous matter.[14−16]

Carbonaceous aerosols typically range from 0.001 to 10 $\mu$m in diameter.[11] Although they make up a significant number fraction (up to 50%) of all atmospheric particulate material, particularly in urban environments,[17,18] their formation mechanisms are complex, difficult to measure, and not well understood.[19] Production of carbon-containing particulates is dominated by ground-level anthropogenic combustion processes such as biomass or fossil fuel burning in addition to the minor natural sources such as photochemical oxidation reactions of hydrocarbons or direct vegetation emissions.[20,21] Carbon aerosol particles are also directly injected in the upper troposphere as aircraft-generated soot, and the large surface area they contribute may be responsible for significant heterogeneous chemistry. Such particles may be involved in a net atmospheric cooling effect on climate (either directly by scattering or absorption of radiation or indirectly as cloud condensation nuclei).

Primary combustion-generated carbon aerosol is also known as soot. Soot has been defined as consisting of an adsorbed soluble organic fraction, and an insoluble core that is resistant to oxidation.[21] The insoluble component has been variously termed elemental, graphitic or black carbon and there is evidence that this component contains a graphite-like microcrystalline structure,[22] possibly surrounded by a liquidlike hydrocarbon layer.[23] The accepted structure of elemental carbon aerosols is based on small crystallites of impure graphite arranged into a three-dimensional (sometimes fractal) arrangement with a large total surface area and low density.[10]

Our laboratory is interested in the adsorption and photochemistry of small atmospherically relevant organic molecules on carbonaceous surfaces, using graphite and other substrates as models for carbonaceous particulate matter. In this paper, we present an initial study of the adsorption and photochemistry of 1,3-butadiene on graphite. During UV irradiation at wavelengths from about 170 to 270 nm, gaseous 1,3-butadiene generates a variety of species including hydrogen, acetylene, ethylene, ethane, 1-butyne, 1,2-butadiene and polymers. Photolysis of solutions of butadiene produce cyclobutene, bicyclo-[1.1.0]butane, a $C_8H_{16}$ dimer, and polymers.[24] Butadiene has also been shown to polymerize on surfaces.[25,26] It is listed as a "hazardous air pollutant" by the Clean Air Act of 1990 and is a known carcinogen with a threshold limit value of 10 ppm.[27] It enters the atmosphere by similar routes to particulate carbon from forest fires, automobile and truck exhaust or other combustion sources.[28,29] Once in the atmosphere, butadiene can react with species such as $O_3$, OH, $NO_3$, and Cl to form a variety of oxidation products.[28,30]

Ultraviolet irradiation of butadiene is also known to cause isomerization. The majority species in gas phase 1,3-butadiene corresponds to the *s-trans* conformation. Rotation about the single bond generates a higher energy minority species, the spectroscopy and conformation of which have been debated in the literature.[31−36] A consensus seems to be forming that the high energy conformer is a nonplanar *s-gauche* rotamer rather than a planar *s-cis* rotamer. The high energy species can be generated by UV irradiation of the trans species in Ar matrices[31,32] or by deposition of hot vapor onto cooled surfaces.[37,33] There is some evidence that the conformation of the condensed molecule is very close to planar,[31,33] although Szalay et al have commented that the molecule is very floppy

* To whom correspondence should be addressed.

10.1021/jp021196n CCC: $22.00 
Published on Web 09/12/2002

and gas phase and matrix measurements are not necessarily conflicting.[38]

In this work, we apply ultrahigh vacuum techniques to a characterization of the adsorption and photochemistry of butadiene on graphite. Vibrational spectroscopy allows us to tentatively identify the surface species conformation as *s-trans* and the adsorption geometry as parallel to the surface plane. Additionally, we have probed the effect of UV irradiation at both high and low fluences for 193, 248, and 351 nm. At high incident powers ($>10$ mJ/cm$^2$·pulse) we observe laser-induced thermal desorption but at low powers we observe no photon-induced chemistry.

## Experimental Section

All experiments were carried out in a stainless steel ultrahigh vacuum (UHV) chamber that has been described previously.[39] Briefly, the chamber contained a molecular leak valve, a quadrupole mass spectrometer, a X-ray source and hemispherical electron energy analyzer for X-ray photoelectron spectroscopy (XPS), and a high-resolution electron energy loss spectrometer (EELS). The base pressure of the chamber was $1.4 \times 10^{-10}$ Torr.

Highly ordered pyrolytic graphite (HOPG) (grade SPI-2, SPI Supplies) with approximate dimensions of $10 \times 10 \times 1$ mm$^3$ was fastened to a molybdenum sample mount using molybdenum clips. Before introduction to the UHV chamber, the HOPG sample was repeatedly peeled using adhesive tape until an optically flat surface was obtained. An E-type thermocouple was placed between the HOPG front face and one of the molybdenum clips. It was possible to cool the sample to $\geq 80$ K using liquid nitrogen or heat the sample to $\sim$800 K via a tungsten filament embedded in the molybdenum sample mount. Following bakeout, the sample was annealed to 700 K for several hours until a constant surface composition was measured by XPS. After annealing, the HOPG surface was free of detectable contaminants except for the presence of $<0.5\%$ oxygen species that could not be removed.

An excimer laser (Questek 2440) operating at 193 nm (ArF), 248 nm (KrF) or 351 nm (XeF) was used to provide UV photons. The laser was operated at a repetition rate of 5 Hz with average powers up to 100 mJ/cm$^2$·pulse as measured by a calibrated thermopile detector placed at the laser-to-sample distance. The laser pulse duration (fwhm), quoted by the laser manufacturer, was 8−16 ns. The laser light passed through a quartz window on the UHV chamber and impinged the sample at 45° from surface normal. The beam was apertured so that only the sample surface was irradiated. All irradiation experiments were performed at surface temperatures of 83−85 K, and the bulk temperature rise detected by the thermocouple during all irradiation experiments was $\leq 0.5$ K.

1,3-Butadiene vapor (Aldrich 99%) was used without further preparation. The gas was introduced to the UHV chamber via a passivated stainless steel manifold coupled to a molecular leak valve. The gas was dosed onto the sample through a 1/8" inside diameter stainless steel tube (a "directed doser"). To expose the sample consistently, the leak valve was opened with the sample removed from the gas source and mass 39 ($C_3H_3^+$), the most abundant ion in the gas-phase cracking pattern of butadiene, was measured with the mass spectrometer. Once a predetermined and constant signal was obtained, the sample was placed in front of the directed doser ($\sim$5 mm from the sample surface) for a specified amount of time. In separate experiments, we have estimated that the local pressure experienced by the sample in such a dosing arrangement is approximately 250−300 times greater than simple background dosing.

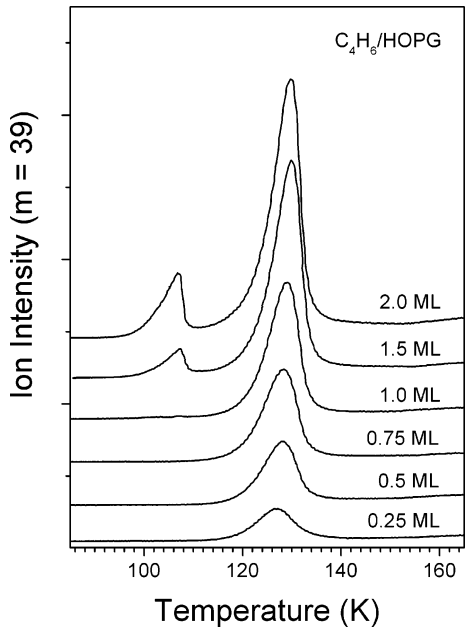


**Figure 1.** TPD profiles for 1,3-butadiene adsorbed on HOPG at 85 K. One monolayer (1 ML) is defined here as the maximum exposure that does not produce multilayer desorption features.

Temperature programmed desorption (TPD) experiments were performed by positioning the graphite surface in line-of-sight of the 2 mm diameter entrance aperture of a shrouded quadrupole mass spectrometer. The electron impact ionization source was operated at 70 eV and a bias of $>-70$ V was placed on the sample in order to repel any electrons escaping from the ion source. During TPD, the sample was heated at a linear rate of 3.5 K/s up to a maximum temperature of 450 K. Occasional experiments performed with maximum temperatures of up to 700 K produced identical results. A fresh exposure of butadiene was prepared for each experiment.

The adsorption and photochemistry of butadiene was also monitored using EELS. The incidence angle was $\theta_i = 55°$ from the surface normal and all data presented in this study was collected 1−3° off-specular ($\theta_s = 56-58°$) to reduce the inelastic background from the semi-metallic graphite surface. The intensity of this inelastic background decreases quickly as the scattering geometry moves away from the specular direction for HOPG.[40] The primary beam energy was 6.1 eV and resolution from the $C_4H_6$/HOPG surface was between 36 and 44 cm$^{-1}$ (4.5−5.5 meV) as determined from the elastic peak fwhm for all data shown here.

## Results

The adsorption of butadiene on HOPG(0001) was initially studied using TPD. Figure 1 shows TPD ($m = 39$, $C_3H_3^+$) profiles for various exposures of butadiene adsorbed on HOPG at 83−85 K. The first monolayer displays apparent first-order desorption kinetics and desorbed with a maximum rate at a temperature, $T_p$, of about 128 K. Using Redhead analysis,[41] the desorption energy was determined to be 32 kJ/mol, suggesting that butadiene was physisorbed on the HOPG surface with minimal intermolecular interaction between the adsorbates. With increased butadiene exposure, a second feature appeared, initially located with $T_p$ at about 106 K. We ascribe this feature to second and multilayer desorption since it did not saturate at large exposures and showed zero-order desorption kinetics. The activation energy of desorption, determined by leading edge analysis,[42] was 28.5 kJ/mol. Interestingly, the monolayer peak

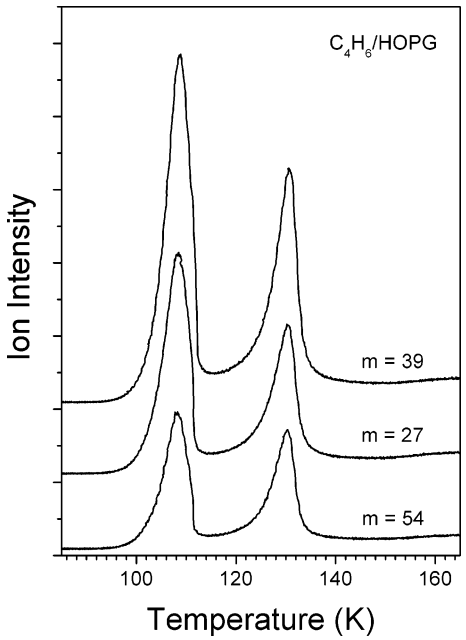


**Figure 2.** TPD profiles for 3.0 ML of 1,3-butadiene on HOPG measured at several fragment masses. The features are in the correct intensity ratio for molecular desorption.

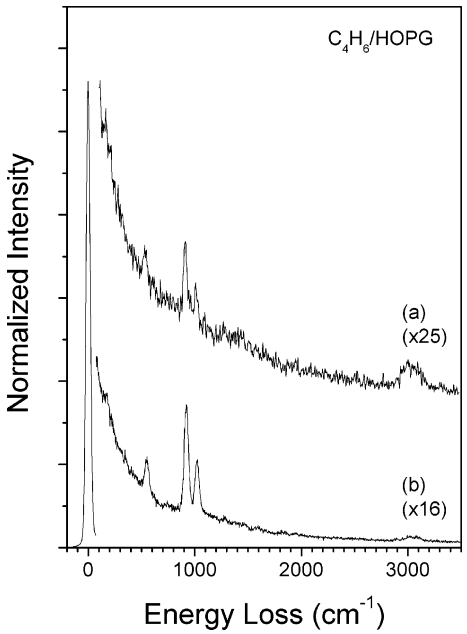


**Figure 3.** Electron energy loss (EEL) spectra of (a) 1.0 ML and (b) 3.0 ML of 1,3-butadiene on HOPG measured 2° off-specular. Vibrational features correspond to molecular *s-trans*-1,3-butadiene adsorbed with its figure axis parallel to the surface plane. The large background is intrinsic to EEL spectra of graphite.[40]

did not saturate as the multilayer peak began to grow in. When the monolayer peak saturated, approximately 16% of the total number of adsorbed molecules were associated with the multilayer peak. This indicates that butadiene was likely forming 3-D islands on the HOPG(0001) surface before the monolayer was complete. Therefore, in this work we define one monolayer (1 ML) as the maximum coverage of butadiene on HOPG where no multilayer desorption was seen by TPD. This coverage represents approximately 84% of the saturated monolayer coverage.

To confirm butadiene desorbed molecularly during TPD, further experiments were performed. Figure 2 shows TPD profiles for several butadiene masses ($m = 39$ $C_3H_3^+$, $m = 27$ $C_2H_3^+$, and $m = 54$ $C_4H_6^+$) at a constant coverage of 3.0 ML. The area under each desorption peak was calculated and compared to the relative intensity for each mass in the cracking pattern of $C_4H_6$(g) determined under our experimental conditions (data not shown). In the mass spectrum of $C_4H_6$(g), $m = 39$ forms the base peak and the relative intensities of $m = 27$ and $m = 54$ fragments were 80 ± 2% and 55 ± 2% of this intensity, respectively. The measured TPD data corresponded closely with the $C_4H_6$(g) cracking pattern with $m = 27$ and $m = 54$ peaks of 75 ± 2% and 51 ± 2% of the $m = 39$ peak intensity, respectively. The similarity of the gas phase and desorbed molecule fragmentation patterns indicated no measurable dissociative adsorption occurred at any of the coverages investigated here (<10 ML).

Figure 3a shows the EELS spectrum for 1.0 ML of butadiene adsorbed on HOPG at 83−85 K. Assignment of the loss features was made by comparison with IR data in the literature.[43] The features visible in the EEL spectra of 1,3-butadiene(ad)/HOPG were the $\tau$(C−C) (torsion between $C_2$ and $C_3$) at ∼186 cm$^{-1}$ (unresolved), the $\tau(CH_2)$ twist at 532 cm$^{-1}$, the $\chi(CH_2)$ wag at 909 cm$^{-1}$, the $\chi$(CH) wag at 1014 cm$^{-1}$, and the $\nu(CH_2)$ stretch region at about 3025 cm$^{-1}$. All of the observed losses in the EEL spectrum belong to out-of-plane ($A_u$ symmetry) vibrations except for the $\nu(CH_2)$ modes. These assignments suggests that planar butadiene adsorbs with its figure axis parallel to the HOPG surface plane and without significant C atom rehybrization. We believe that the appearance of the $\nu(CH_2)$ mode is due to slight lowering of the symmetry of the molecule from $C_{2h}$ due to weak surface bonding. This moves C−H motion away from parallel to the surface plane and allows it to be observed by EELS. Furthermore, it is known that C−H modes are strongly impact active in EELS.[44] The slight off-specular measurement strategy adopted here will increase our sensitivity to these modes. The proposed butadiene adsorption geometry was also supported by the absence of several strong in-plane IR active molecular vibrations (for example, the $\nu_o$(C═C) stretch at 1643 cm$^{-1}$ and the $\delta$(═$CH_2$) scissor bend at 1441 cm$^{-1}$). These modes do become visible in large off-specular measurements (14−20° off-specular, data not shown). There was no evidence for the formation of cyclic-type adsorbates on graphite as have been proposed on some metal surfaces where strong interaction between the butadiene and the surface leads to significant double bond activation.[45]

The frequencies of the modes observed in our EEL spectra most closely match those measured for the *s-trans* conformer (rotamer) of 1,3-butadiene.[35] The frequency shifts associated with *trans-gauche-cis* isomerization in butadiene are generally small for the $A_u$ modes visible in our EEL spectra. However, the $\tau(CH_2)$ twisting mode appears at 524 cm$^{-1}$ in *s-trans*-1,3-butadiene but at >700 cm$^{-1}$ in both the *s-gauche* and *s-cis* forms. Therefore, we tentatively believe that the average molecular conformation corresponds with the *trans*-isomer. The *s-trans* form is the thermodynamically most stable isomer of $C_4H_6$(g) by about 12 kJ/mol.[36] At room temperature, about 4% of gaseous butadiene molecules are in the high energy conformation[46] but this value will be significantly smaller (∼$10^{-5}$%) if fully equilibrated at the temperatures corresponding to that of the HOPG surface (83−85 K). Similar conclusions about the adsorption geometry and conformation of butadiene on Au(111) were reached in previous studies by reflection−absorption infrared spectroscopy.[47]

Electron energy loss spectroscopy was also used to investigate multilayer (3.0 ML) adsorption of butadiene on HOPG, as shown in Figure 3b. The multilayer data was very similar to

**TABLE 1: Vibrational Frequencies Measured by EELS for 1,3-butadiene(ad)/HOPG**

| assignment | EELS 1 ML/HOPG ($cm^{-1}$) | EELS 3 ML/HOPG ($cm^{-1}$) | EELS $h\nu$ + 3ML/HOPG ($cm^{-1}$)[a] | IR Ar matrix/(g) ($cm^{-1}$)[b] |
|---|---|---|---|---|
| $\tau$(C−C) torsion | ∼186 | ∼186 | | 162 |
| $\tau(CH_2)$ twist | 532 | 550 | 542 | 524 |
| $\chi(CH_2)$ wag | 909 | 919 | 913 | 908 |
| $\chi$(C−H) wag | 1014 | 1021 | 1016 | 1014 |
| $\nu_s(CH_2)$, $\nu$(C−H) stretch | 3025[c] | 3043[c] | 3027[c] | 3013 |
| $\nu_a(CH_2)$ stretch | | | | 3100 |

[a] Cumulative energy of 0.3 W/cm² at 100 mJ/cm²·pulse, $\lambda$ = 193 nm. [b] For *s-trans*-1,3-butadiene.[35] [c] Unresolved.

the monolayer data but with an increased signal-to-noise ratio. All of the peaks appeared at approximately the same frequency as in the monolayer. No new peaks were apparent in the multilayer spectrum and the ratio of intensities between the various features was very similar to that of the monolayer. We believe that these data indicate that butadiene forms multilayers on top of the first monolayer, with a similar "parallel" adsorption geometry to that of the monolayer. The peak maxima for all EELS data are listed in Table 1.

Figure 4 shows TPD results ($m$ = 39) for 1.0 ML (Figure 4 (a)) and 3.0 ML (Figure 4(b)) of butadiene adsorbed on HOPG following irradiation with 193 nm photons at an average incident energy of 100 mJ/cm²·pulse. Irradiation decreased the butadiene coverage as clearly seen in Figure 4a where, after irradiating the butadiene monolayer with a total of 51.3 J/cm² ($5 \times 10^{19}$ photons/cm²), only 18% of the initial $C_4H_6$ remained on the surface. The peak shape and $T_p$ remained constant for all TPD data collected. Furthermore, mass spectra from $m$ = 0−100 collected during TPD showed no measurable desorbing fragments other than those attributable to molecular butadiene.

Figure 4b shows the same data as for Figure 4a but for an initial coverage of 3.0 ML of butadiene on HOPG. Irradiation of the adsorbate layers produced a decrease in the $m$ = 39 signal for both monolayer and multilayer peaks. Measurements at other fragment masses confirmed that, as for 1 ML, the only significant species remaining on the surface following irradiation was butadiene. The multilayer peak intensity decreased at a faster rate than the monolayer peak intensity, as will be discussed further below. There was no evidence for reaction products remaining adsorbed, implying that butadiene either desorbed molecularly from the surface during irradiation or produced small product molecules that had sufficient thermal or kinetic energy to desorb. Attempts to directly monitor products expelled from the surface during irradiation were unsuccessful due to saturation of the mass spectrometer multiplier during the laser pulse.

For both monolayer and multilayer coverages, the fraction of butadiene desorbed followed an exponential dependence with cumulative incident energy (first-order desorption kinetics). The apparent cross-section for photodesorption, $\sigma$, was calculated to be $3.3 \times 10^{-20}$ cm²/molecule·photon from the monolayer TPD peak and $1.0 \times 10^{-17}$ cm²/molecule·photon from the multilayer peak at 193 nm and 100 mJ/cm²·pulse. The cross-section for desorption from the monolayer was approximately constant, whether calculated from 1.0 or 3.0 ML postirradiation TPD. Similar values were calculated for 248 and 351 nm incident light at the same incident power. However, as discussed in below, the effective cross section was found to depend strongly on the laser fluence, indicating that the decrease in butadiene coverage with irradiation was not due to simple photodesorption.

Electron energy loss spectroscopy was used to examine the 193 nm photochemistry of 1.0 and 3.0 ML of 1,3-butadiene on HOPG. For all cumulative incident energies up to 50 J/cm², identical features to those observed for the unirradiated adlayers, shown in Figure 3, were observed (data not shown). The absolute intensity of all peaks decreased with increasing incident energy, consistent with simple molecular desorption of the 1,3-butadiene. No new peaks appeared in the EELS data with

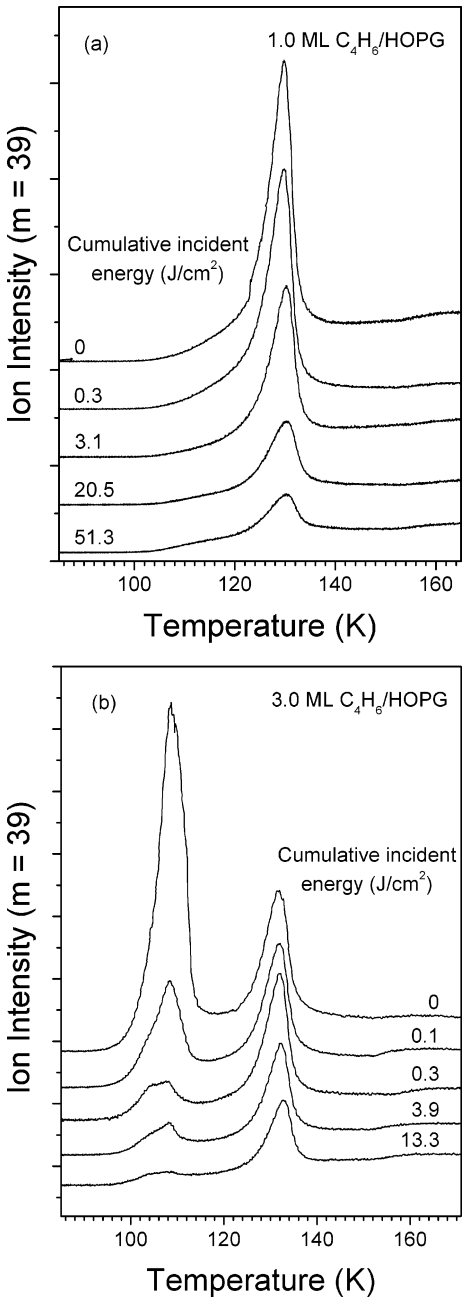


**Figure 4.** Temperature programmed desorption profiles for (a) 1.0 ML and (b) 3.0 ML of 1,3-butadiene irradiated with 193 nm photons at 100 mJ/cm²·pulse incident energies for various total cumulative incident energies. Note the decreases in peak intensity for monolayer and multilayer features with irradiation.

prolonged irradiation, suggesting that adsorbed state reaction products were not created in measurable quantities and in accord with the TPD data discussed above.

Over the past 15 years, several mechanisms leading to the desorption of molecules during photon irradiation have been proposed in the literature. The three general phenomena that have emerged as important are (1) an adsorbate-mediated process, commonly called photodesorption or photoejection, involving the direct absorption of a photon by an adsorbate molecule or adsorbate−substrate complex; (2) a substrate-mediated process involving the absorption of a photon by the surface and electronic energy transfer to the adsorbate−substrate bond; and (3) laser-induced thermal desorption (LITD) which occurs when energy absorbed by the surface is rapidly converted to surface phonons and the local surface temperature rise causes thermal desorption. For a more detailed discussion of these mechanisms, the reader is referred elsewhere.[48−50] The characteristics of the data presented here for molecular desorption of 1,3-butadiene adsorbed on HOPG are best described by a laser-induced thermal desorption mechanism.

Laser-induced thermal desorption (LITD) is a consequence of exposing an adsorbate-covered surface to a large absorbed photon flux through pulsed laser irradiation. Excited electrons generated within the optical penetration depth of the surface decay rapidly (on the order of $10^{-12}$ s) via creation of phonons (thermal energy). This energy diffuses away from the irradiated region both during and following cessation of the laser pulse until thermal equilibrium is reestablished. Depending upon the optical and thermal properties of the solid, it is possible to locally heat the surface at rates corresponding to more than $10^{11}$ K/s.[51]

The temperature rise of a surface can be estimated using equations in the literature for a LITD model that simplifies the Gaussian temporal profile of the laser to a triangular pulse.[52] We have used this model to estimate the transient temperature of the surface when irradiated by UV light under the conditions described above. The energy absorbed by the surface was estimated from the incident power density, the optical absorption coefficient of graphite ($1.7 \times 10^5$ cm$^{-1}$ at 193 nm, $3.6 \times 10^5$ cm$^{-1}$ at 248 nm, and $2.5 \times 10^5$ cm$^{-1}$ at 351 nm[53]) and the reflectivity of the surface in the experimental geometry (calculated from the Fresnel equations as 0.013 at 193 nm, 0.05 at 248 nm, and 0.068 at 351 nm). The rate of heat flow away from the irradiated area was estimated from the average thermal conductivity, K, of graphite (28.6 W/cm·K at 80 K[27]) and the thermal diffusivity (127.8 cm$^2$/s at 80 K, calculated from $K/(\rho \cdot C_p)$ where $\rho$ is the density and $C_p$ the specific heat capacity[54] of graphite).

The results of the calculation give an estimate of the change in surface temperature versus time. A representative temperature profile is presented in Figure 5 for a 193 nm, 12 ns fwhm laser pulse of 100 mJ/cm$^2$.[55] The maximum temperature rise, $\Delta T$, under these conditions was 157 K. The estimated $\Delta T$ was 149 K for 248 nm and 146 K for 351 nm incident light, similar to that for 193 nm largely because of the relatively uniform absorption coefficient of graphite over this wavelength range. At all three wavelengths, irradiation produces surface temperatures considerably above the temperature for the onset of desorption for monolayer (∼105 K) and multilayer (∼95 K) butadiene. Indeed, transient surface temperatures up to about 240 K can be produced during irradiation under these conditions.

Despite the simplicity of the model, the accuracy of the calculated surface temperature rise and onset of laser-induced thermal desorption measured in TPD experiments appears to be good. For example, the desorption of 1 ML of butadiene

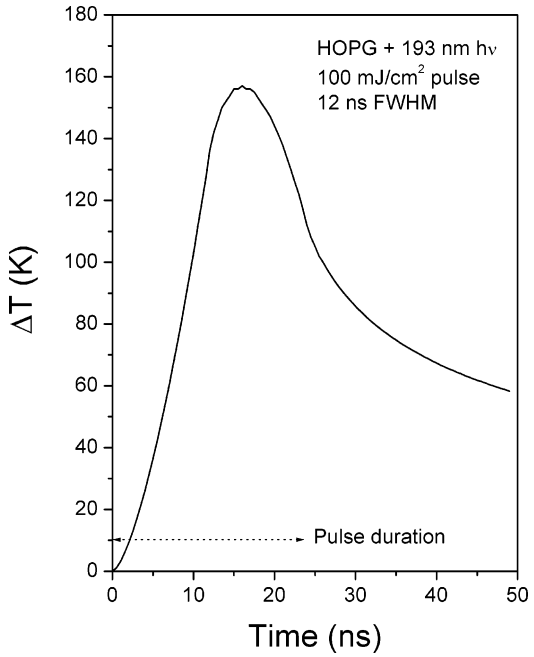


**Figure 5.** Calculated surface temperature rise, $\Delta T$, for HOPG using a triangular approximation for the temporal profile of a 100 mJ/cm$^2$ 193 nm laser pulse.[52]

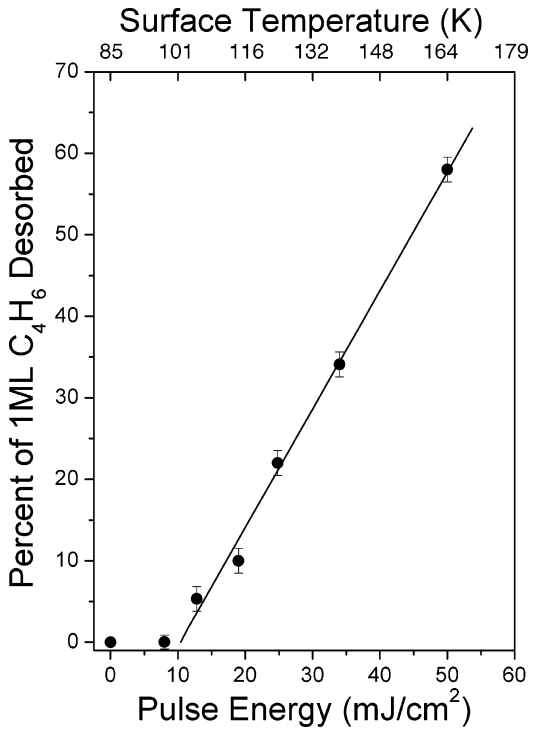


**Figure 6.** The percentage of 1.0 ML of 1,3-butadiene desorbed from HOPG as a function of incident laser pulse energy up to 50 mJ/cm$^2$·pulse. The line is a linear fit to the data points between 12 and 50 mJ/cm$^2$·pulse. Also shown is the calculated transient surface temperature maximum (85 K + $\Delta T$).

was followed under conditions of variable incident flux for 193 nm UV irradiation at between 0 and 50 mJ/cm$^2$·pulse. In these experiments, the total amount of energy deposited onto the surface was fixed at 10.3 J/cm$^2$. The percentage of the monolayer desorbed by irradiation was evaluated by postirradiation TPD measurements and the results are shown in Figure 6. At low pulse energies of 12 mJ/cm$^2$·pulse, only about 5% of the monolayer was desorbed after a total energy of 10.3 J/cm$^2$ had been deposited on the HOPG surface. However, at a pulse

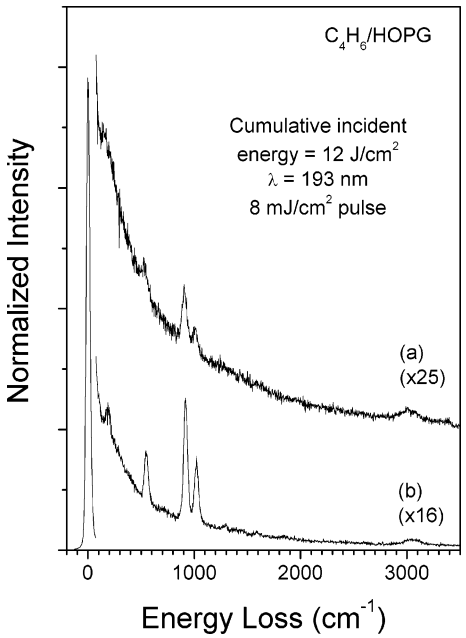


**Figure 7.** Electron energy loss spectrum for initial coverages of (a) 1.0 and (b) 3.0 ML 1,3-butadiene irradiated with 193 nm photons at 8 mJ/cm$^2$·pulse for a total cumulative energy of 12 J/cm$^2$.

energy of 50 mJ/cm$^2$·pulse, approximately 57% of the monolayer was desorbed after a total energy of 10.3 J/cm$^2$ had been incident on the surface. The percentage of the monolayer desorbed followed an approximately linear dependence with pulse energy in the range of 12−50 mJ/cm$^2$·pulse. Similar behavior for the desorbed fraction as a function of incident laser power was calculated by Burgess et al.[52] In our case, the intercept for 0% desorption occurred at a pulse energy of 10.5 mJ/cm$^2$·pulse, corresponding to a calculated $\Delta T$ of 16 K and a transient surface temperature up to about 101 K, comparable to the measured onset for monolayer desorption (105 K). Clearly, the more rapid desorption of multilayer versus monolayer butadiene(ad)/HOPG, as observed in Figure 4b, must be related to the lower temperature for the onset of desorption.

Irradiation experiments were also conducted using 193, 248 and 351 nm laser pulses with energies of less than the 10 mJ/cm$^2$·pulse threshold observed for the onset of LITD of monolayer 1,3-butadiene(ad)/HOPG. For example, the calculated transient surface temperature maximum for irradiation using 8 mJ/cm$^2$·pulse was about 95 K, comparable with the temperature onset of multilayer desorption. Figure 7 shows the EEL spectra obtained after 193 nm irradiation of both 1.0 and 3.0 ML of butadiene adsorbed of HOPG at a total incident energy of 12 J/cm$^2$ at 8 mJ/cm$^2$·pulse. These electron energy loss spectra were essentially identical to those shown in Figure 3 and corresponded to molecularly adsorbed $C_4H_6$. In fact, some multilayer desorption does occur under these UV irradiation conditions and the final coverage of the initial 3.0 ML corresponded to approximately 2.1 ML. Post-irradiation TPD experiments revealed that little monolayer desorption occurred at any wavelength using incident powers of 8 mJ/cm$^2$·pulse. Importantly, no new EELS-active photoreaction products were detected, even after prolonged UV exposures of up to 50 J/cm$^2$. Hence, we conclude that no observable photochemistry takes place in the adsorbed monolayer under low fluence conditions.

## Discussion

Gas-phase butadiene absorbs UV radiation from about 170 nm to >270 nm. The gas-phase absorption cross-sections for butadiene are $\sim 4 \times 10^{-17}$ cm$^2$, $\sim 2 \times 10^{-19}$ cm$^2$ and essentially zero at 193, 248, and 351 nm, respectively.[56] Near 200 nm, absorption results in a $\pi^* \leftarrow \pi$ transition from the $1A_g$ ground state to an excited $1B_u$ state. The molecule rapidly (~50 fs) crosses to a slightly lower energy "doubly excited" $2A_g$ state and branches to products or reactants at a conical intersection with the ground state.[57] There is recent computational evidence that both in-place and out-of-plane motions are important at the conical intersection.[58] Return to the ground state takes about 100 fs and isomerization from *trans*- to *cis*-1,3-butadiene may also occur on the hot ground state in about 270 fs at an excess energy of 6.2 eV.[57]

Early experiments indicated that 1,3-butadiene photopolymerizes under UV light in the presence of a surface,[25,26] although it is likely that gas phase species participate in that process. Photolysis of solutions of butadiene in cyclohexane produces mostly cyclobutene and minor quantities of products such as bicyclo[1.1.0]butane, $C_8H_{16}$ dimer, and a polymer.[24] Photolysis of gas-phase butadiene produces hydrogen, acetylene, ethylene, ethane, 1-butyne, 1,2-butadiene, and polymer.[24] Absence of any reaction in the adlayer is surprising in view of the reports of varied photochemistry for the gaseous molecule. For example, Arnold and co-workers[33] have successfully used 214 nm light to generate and stabilize the minority butadiene conformer in 10 K Ar matrices. This wavelength is near the center of the absorption band for the *trans* isomer,[36] but the envelope extends to below 200 nm and can be excited by our 193 nm laser light. As such, if the potential energy surfaces of the adsorbate are not significantly perturbed by surface bonding, we might reasonably expect to observe photoisomerization of the majority *trans* isomer into the *s-gauche* or *s-cis* isomer at 193 nm.

In fact, photoisomerization of *s-trans* to *s-cis*-(or *gauche*-)1,3-butadiene adsorbed on HOPG may occur in our experiments but remain undetected if the conversion from the photogenerated *cis* or *gauche* back to the *trans* form is facile. Photon-stimulated reconversion does not appear to occur at wavelengths <200 nm since the *cis* isomer does not absorb in this region: the *cis* isomer absorbs at slightly longer wavelengths ($\lambda_{max}$ = 226 nm in Ar matrix, 216 nm in (g))[35] than the *trans*. In contrast, it is believed that irradiation in the 237−249 nm region exclusively excites the minority *cis* form and photoconverts any minority species to the *trans* form.[31,33] Therefore, we would not expect to observe the *cis/gauche* product when irradiating at 248 nm. However, it is the rapid disappearance of bands associated with minority species generated in Ar matrices warmed above 60 K[31] that suggests that reconversion of any photogenerated *cis/gauche* conformer to the *trans* form may occur thermally at the surface temperature of our experiments. As such, the equilibrium minority species surface concentration would remain too small to be detected by our vibrational spectroscopy.

Even with facile thermal reconversion at 83−85 K, we might expect the excited state of butadiene prepared by UV light to live long enough for other products to be produced via branching at the $2A_g$/ground-state conical intersection mentioned above. An absence of photochemistry for a molecule adsorbed on a surface has been associated with excited-state quenching by the large density of proximal electronic states. For example, photolysis of $CH_3I$ is significantly inhibited for a monolayer adsorbed on Pt(111).[59] Since the lifetime of the excited-state butadiene molecule is less than 100 fs,[57] lack of any photochemistry implies that the quenching process can successfully compete with reaction on this time scale. Excited state lifetimes for adsorbed molecules are approximately 1−100 fs,[60,61] with resonant processes forming the quickest part of this range.

Despite the relatively weak bonding between butadiene and HOPG, energy exchange from butadiene to HOPG appears to be efficient. Of course, rapid quenching of the excited state would also explain the absence of the *s-cis/gauche* rotamer in our vibrational spectra without the need to invoke a thermal reconversion process.

## Conclusions

The adsorption and photochemistry of butadiene ($C_4H_6$) on HOPG(0001) has been investigated. At <85 K, butadiene adsorbs on HOPG probably forming 3-D islands on the surface as indicated by the appearance of multilayer TPD features before saturation of the first adsorbed layer. Temperature programmed desorption suggests that butadiene is physisorbed on the HOPG surface with a monolayer desorption energy of 32 kJ/mol. Electron energy loss spectroscopy suggests that the figure axis of the molecule is parallel to the surface plane and that multilayers adsorb with approximately the same geometry as the first layer. The features of the EEL spectra can be assigned to *s-trans* butadiene.

Irradiation of both 1 and 3 ML coverages of $C_4H_6$/HOPG-(0001) by UV photons at fluences up to 100 mJ/cm$^2$•pulse induces molecular photodesorption by a laser-induced thermal desorption mechanism. At lower energies of (<10 mJ/cm$^2$• pulse), no photodesorption or other photochemistry was measured by TPD or EELS. The lack of photochemistry implies that the excited state prepared by photon absorption by 1,3-butadiene is quenched in less than 100 fs. Alternatively, it is possible that photoisomerization occurs at 193 nm, but that rapid reconversion of the *s-cis/gauche* species to the more stable *s-trans* rotamer is facile at 83−85 K.

## References and Notes


(1) Molina, M. J.; Tso, T.-L.; Molina, L. T.; Wang, F. C.-Y. *Science* **1987**, *238*, 1253.

(2) Tolbert, M. A.; Rossi, M. J.; Malhotra, R.; Golden, D. M. *Science* **1987**, *238*, 1258.

(3) Chu, L. T.; Leu, M.-T.; Keyser, L. F. *J. Phys. Chem.* **1993**, *97*, 12798−12804.

(4) Barone, S. B.; Zondlo, M. A.; Tolbert, M. A. *J. Phys. Chem. A* **1997**, *101*, 8643.

(5) Berland, B. S.; Tolbert, M. A.; George, S. M. *J. Phys. Chem. A* **1997**, *101*, 9954.

(6) Zondlo, M. A.; Barone, S. B.; Tolbert, M. A. *J. Phys. Chem. A* **1998**, *102*, 5735.

(7) Graedel, T. E.; Crutzen, P. J. *Atmospheric Change. An Earth System Perspective*; W. H. Freeman and Company: New York, 1993.

(8) Molina, M. J.; Molina, L. T.; Kolb, C. E. *Annu. Rev. Phys. Chem.* **1996**, *47*, 327.

(9) Peter, T. *Annu. Rev. Phys. Chem.* **1997**, *48*, 785.

(10) Seinfeld, J. H.; Pandis, S. *Atmospheric Chemistry and Physics: Air Pollution and Climate Change*; Wiley-Interscience: New York, 1997.

(11) Brasseur, G. P.; Orlando, J. J.; Tyndall, G. S. *Atmospheric Chemistry and Global Change*; Oxford University Press: New York, 1999.

(12) Finlayson-Pitts, B. J.; Pitts Jr., J. N. *Chemistry of the Upper and Lower Atmosphere*; Academic Press: San Diego, 2000.

(13) Zondlo, M. A.; Hudson, P. K.; Prenni, A. J.; Tolbert, M. A. *Annu. Rev. Phys. Chem.* **2000**, *51*, 473.

(14) Choi, W.; Leu, M.-T. *J. Phys. Chem. A* **1998**, *102*, 7618.

(15) Finlayson-Pitts, B. J.; Hemminger, J. C. *J. Phys. Chem. A* **2000**, *104*, 11463.

(16) Grassian, V. H. *Int. Rev. Phys. Chem.* **2001**, *20*, 467.

(17) Novakov, T.; Hegg, D. A.; Hobbs, P. V. *J. Geophys. Res.* **1997**, *102*, 30023.

(18) Lary, D. L.; Shallcross, D. E.; Toumi, R. *J. Geophys. Res.* **1999**, *104*, 15929.

(19) Homann, K.-H. *Angew. Chem., Int. Ed. Engl.* **1998**, *37*, 2434.

(20) Liousse, C.; Penner, J. E.; Chuang, C.; Walton, J. J.; Eddelman, H.; Cachier, H. *J. Geophys. Res.* **1996**, *101*, 19411.

(21) Penner, J. E.; Novakov, T. *J. Geophys. Res.* **1996**, *101*, 19373.

(22) Rosen, H.; Novakov, T. *Nature* **1977**, *266*, 708.

(23) McDow, S. R.; Jang, M.; Hong, Y.; Kamens, R. M. *J. Geophys. Res.* **1996**, *101*, 19593.

(24) Haller, I.; Srinivasan, R. *J. Chem. Phys.* **1964**, *40*, 1992.

(25) White, P. *Proc. Chem. Soc.* **1961**, 337.

(26) Wright, A. N. *Nature* **1967**, *215*, 953.

(27) Lide, D. R., Ed *CRC Handbook of Chemistry and Physics*, 75th ed.; CRC Press: Boca Raton, FL, 1994.

(28) Tuazon, E. C.; Alvardo, A.; Aschmann, S. M.; Atkinson, R.; Arey, F. *Environ. Sci. Technol.* **1999**, *33*, 3586.

(29) Friedli, H. R.; Atlas, E.; Stroud, V. R.; Giovanni, L.; Campos, T.; Radke, L. F. *Global Biogeochem. Cycles* **2001**, *15*, 435.

(30) Wang, W.; Finlayson-Pitts, B. J. *J. Geophys. Res.* **2001**, *106*, 4939.

(31) Squillacote, M. E.; Sheridan, R. S.; Chapman, O. L.; Anet, F. A. L. *J. Am. Chem. Soc.* **1979**, *101*, 3657.

(32) Furukawa, Y.; Takeuchi, H.; Harada, I.; Tasumi, M. *Bull. Chem. Soc. Jpn.* **1983**, *56*, 392.

(33) Arnold, B. R.; Balaji, V.; Michl, J. *J. Am. Chem. Soc.* **1990**, *112*, 1808.

(34) Wiberg, K. B.; Rosenberg, R. E. *J. Am. Chem. Soc.* **1990**, *112*, 1509.

(35) De Maré, G. R.; Panchenko, Y. N.; Auwera, J. V. *J. Phys. Chem. A* **1997**, *101*, 3998.

(36) Saltiel, J.; Sears, D. F.; Turek, A. M. *J. Phys. Chem. A* **2001**, *105*, 7569.

(37) Huber-Wälchli, P. *Ber. Bunsen-Ges. Phys. Chem.* **1978**, *82*, 10.

(38) Szalay, P. G.; Lischka, H.; Karpfen, A. *J. Phys. Chem.* **1989**, *93*, 6629.

(39) Bryden, T.; Garrett, S. J. *J. Phys. Chem. B* **1999**, *103*, 10481.

(40) Palmer, R. E.; Annett, J. F.; Willis, R. F. *Surf. Sci.* **1987**, *189/190*, 1009.

(41) Redhead, P. A. *Vacuum* **1962**, *12*, 203.

(42) de Jong, A. M.; Niemantsverdriet, J. M. *Surf. Sci.* **1990**, *223*, 355.

(43) Panchenko, Y. N. *Spectrochim. Acta* **1975**, *31A*, 1201.

(44) Ibach, H.; Mills, D. L. *Electron Energy Loss Spectroscopy and Surface Vibrations*; Academic Press: London, 1982.

(45) Weiss, M. J.; Hagedorn, C. J.; Weinberg, W. H. *J. Vac. Sci. Technol. A* **2000**, *18*, 1443.

(46) Wiberg, K. B.; Rosenberg, R. E. *J. Am. Chem. Soc.* **1990**, *112*, 1509.

(47) Osaka, N.; Akita, M.; Itoh, K. *J. Phys. Chem. B* **1998**, *102*, 6817.

(48) Zhou, X. L.; Zhu, X. Y.; White, J. M. *Surf. Sci. Rep.* **1991**, *13*, 73−220.

(49) Ho, W. *Surf. Sci.* **1994**, *299/300*, 996.

(50) Ho, W. *J. Phys. Chem.* **1996**, *100*, 13050.

(51) Brand, J. L.; George, S. M. *Surf. Sci.* **1986**, *167*, 341.

(52) Burgess, D.; Stair, P. C.; Weitz, E. *J. Vac. Sci. Technol. A* **1986**, *4*, 1362.

(53) Borghesi, A.; Guizzetti, G. *Handbook of Optical Constants of Solids 2*; Academic Press: New York, 1991.

(54) DeSorbo, W.; Tyler, W. W. *J. Chem. Phys.* **1953**, *21*, 1660.

(55) It should be noted that our calculation averages the highly anisotropic thermal conductivity of graphite, and uses the average fwhm laser pulse duration specified by the laser manufacturer (12 ns). Surface temperature rises calculated using the longest (16 ns) or shortest (8 ns) fwhm laser pulse specified by the laser manufacturer are approximately 15% lower and 17% higher, respectively, than those quoted here.

(56) Fahr, A.; Nayak, A. K. *Chem. Phys.* **1994**, *189*, 725.

(57) Fuss, W.; Schmid, W. E.; Trushin, S. A. *Chem. Phys. Lett.* **2001**, *342*, 91.

(58) Ostojíc, B.; Domke, W. *Chem. Phys.* **2001**, *269*, 1.

(59) Liu, Z. M.; Akhter, S.; Roop, B.; White, J. M. *J. Am. Chem. Soc.* **1988**, *110*, 8708.

(60) Zhou, X. L.; Zhu, X. Y.; White, J. M. *Surf. Sci. Rep.* **1991**, *13*, 73.

(61) Zimmermann, F.; Ho, W. *Surf. Sci. Rep.* **1995**, *22*, 127−247.